Clin Genet 2016
Printed in Singapore. All rights reserved

CLINICAL GENETICS
doi: 10.1111/cge.12762

Short Report

A homozygous nonsense variant in *IFT52* is associated with a human skeletal ciliopathy

Girisha K.M., Shukla A., Trujillano D., Bhavani G.S., Hebbar M., Kadavigere R., Rolfs A. A homozygous nonsense variant in *IFT52* is associated with a human skeletal ciliopathy.
Clin Genet 2016. © John Wiley & Sons A/S. Published by John Wiley & Sons Ltd, 2016

Intraflagellar transport (IFT) is vital for the functioning of primary cilia. Defects in several components of IFT complexes cause a spectrum of ciliopathies with variable involvement of skeleton, brain, eyes, ectoderm and kidneys. We examined a child from a consanguineous family who had short stature, narrow thorax, short hands and feet, postaxial polydactyly of hands, pigmentary retinopathy, small teeth and skeletal dysplasia. The clinical phenotype of the child shows significant overlap with cranioectodermal dysplasia type I (Sensenbrenner syndrome). Whole-exome sequencing revealed a homozygous nonsense variant p.R142* in *IFT52* encoding an IFT-B core complex protein as the probable cause of her condition. This is the first report of a human disease associated with *IFT52*.

Conflict of interest

None declared.

K. M. Girisha[a], A. Shukla[a], D. Trujillano[b], G. S. Bhavani[a], M. Hebbar[a], R. Kadavigere[d] and A. Rolfs[b,c]

[a]Department of Medical Genetics, Kasturba Medical College, Manipal University, Manipal, India, [b]Department of Bioinformatics, Centogene AG, Rostock, Germany, [c]Albrecht-Kossel-Institute for Neuroregeneration, Medical University Rostock, Rostock, Germany, and [d]Department of Radiodiagnosis and Imaging, Kasturba Medical College, Manipal University, Manipal, India

Key words: chondrodysplasia – ciliopathy – exome sequencing – intraflagellar transport – sensenbrenner syndrome – short rib thoracic dysplasia

Corresponding author: Dr Katta M. Girisha, Department of Medical Genetics, Kasturba Medical College, Manipal University, Manipal 576104, India.
Tel.: +91 820 2923149;
fax: +91 820 2571934;
e-mail: girish.katta@manipal.edu

Received 9 December 2015, revised and accepted for publication 12 February 2016

Human ciliopathies comprise a group of multisystemic genetic disorders caused by mutations in genes required for ciliary assembly and maintenance (1). Defective intraflagellar transport (IFT) due to mutations in genes coding components of kinesin, dynein, IFT-A and IFT-B complexes are associated with a wide variety of human diseases with significant overlapping clinical features. To date all IFT-A and five IFT-B components have been reported to cause human diseases, most of which are skeletal ciliopathies (Table S1, Supporting Information) (2). Mutations in genes encoding components of IFT-B core complex have been previously reported with reno-ocular ciliopathies (3). Here we report the first human skeletal ciliopathy associated with a nonsense variant in *IFT52*, encoding an IFT-B core complex protein.

Materials and methods

Case report

The proband was evaluated at 3 years of age. She was born at term by lower segment cesarean section to consanguineously married parents (Fig. S1). She weighed 3.75 kg (normal) at birth. Bilateral postaxial polydactyly in the hands was noted at birth and was surgically excised. Mild respiratory distress was evident in the immediate newborn period and was managed symptomatically. She had a significant delay of motoric functions. She achieved neck holding at 18 months of age, sat at 2 years and walked without support at two and a half years. Cognitive and language development are age appropriate. She speaks in complete sentences and is toilet trained. She had several episodes of wheezing and

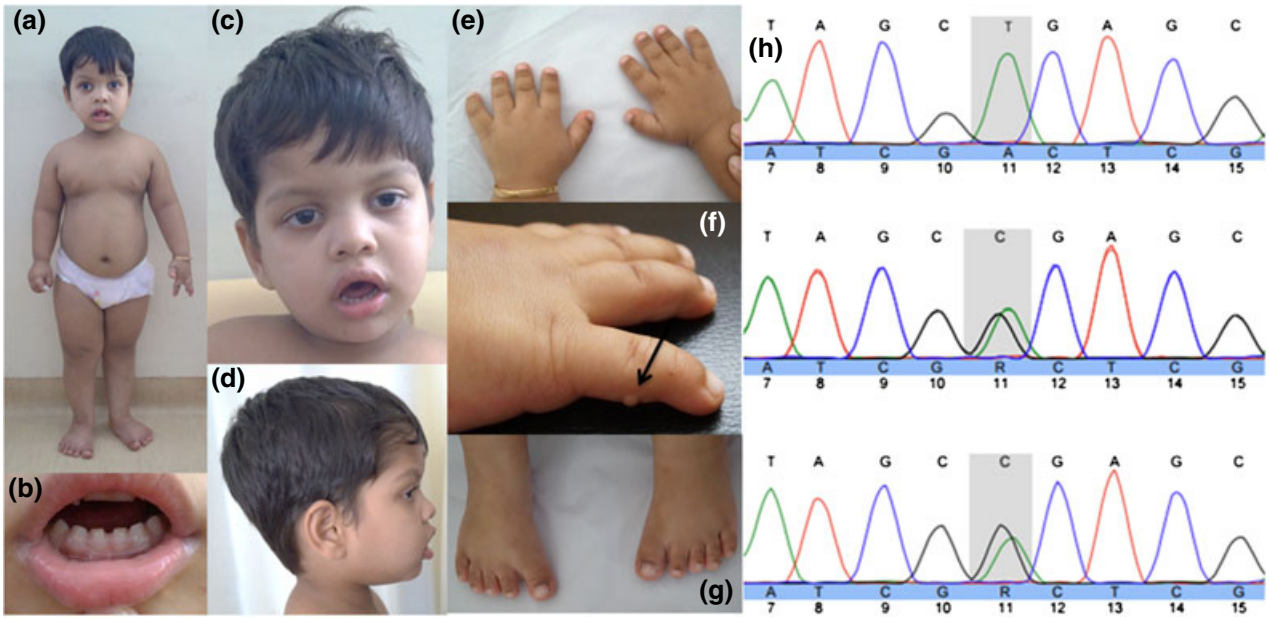

Fig. 1. Proband at 3 years of age has short limbs, narrow thorax, dolicocephaly, tall forehead, telecanthus, mid-face hypoplasia, depressed nasal bridge, thick and everted vermilion of upper and lower lips, small and widely spaced teeth and low set ears (**a–d**). She also has short hands with brachydactyly (**e**) and stump of surgically excised postaxial polydactyly on the right hand (arrow; **f**). Feet show sandal gap and brachydactyly (**g**). Chromatogram of proband shows homozygous nonsense mutation (c.424C > T in *IFT52* NM_016004.3) and heterozygous status in parents for the same (**h**: proband – upper panel, mother – middle panel, father – lower panel).

required bronchodilators. She has progressive deterioration of peripheral vision and now has only central vision.

Her occipito-frontal circumference was 49.5 cm (normal), height 88 cm (normal) and weight 15 kg [+2 standard deviation (SD), 85th centile] as per Center for Disease Control and Prevention growth charts (4). She had dolichocephaly, tall forehead, telecanthus, mid-face hypoplasia, broad and depressed nasal bridge, full cheeks, thick and everted vermilion of the upper and lower lips and low set ears. Her teeth were small, widely spaced and carious. The thorax was short and narrow with a protuberant abdomen. She had short limbs with marked brachydactyly and laxity in both hands and feet. The stumps of surgically excised postaxial polydactyly in hands and sandal gap in feet were noted (Fig. 1). A soft liver was palpable for 3 cm below the right costal margin. Her gait was normal. She had nystagmus. Scalp hair was normal. All other results of the systemic examination were unremarkable.

Radiological survey at 3 years revealed short metacarpals, short metatarsals, short phalanges, cone-shaped epiphysis of phalanges, hypoplastic distal phalanges and striking angel-shaped middle phalanges. A complete hemogram, liver function, renal parameters, urinalysis were unremarkable. Ultrasound imaging of the abdomen revealed normal liver and kidneys. Echocardiography revealed trivial tricuspid regurgitation and mild pulmonary arterial hypertension without any structural malformations. Magnetic resonance imaging of the brain at 6 months of age showed a hypoplastic corpus callosum (Fig. 2). Ophthalmology evaluation revealed hypermetropia and salt and pepper appearance of the fundus suggesting retinal degenerative changes. The visual evoked potential and brainstem evoked response audiometry study were normal. Vineland Social Maturity Scale revealed borderline deficits in social and adaptive functioning. Her karyotype was normal. The parents consented for the study and publication of photographs. The study has the approval of institutional ethics committee. The phenotypic information can be accessed at PhenomeCentral (https://www.phenomecentral.org/P0002186).

Chromosomal microarray

Chromosomal microarray was performed using both copy number changes and single nucleotide polymorphism probes on a whole genome array (Illumina HumanCytoSNP-12, Illumina Inc., San Diego, CA) from the peripheral blood DNA. All data were analyzed and reported using GenomeStudio and KaryoStudio softwares (NCBI human genome build 37.1, hg19) and follows International System for Cytogenetic Nomenclature (ISCN) guidelines.

Exome sequencing

Genomic DNA was extracted from the whole blood using the standard phenol-chloroform method. Genomic capture was carried out with Illumina's Nextera Rapid Capture Exome Kit. Massively parallel sequencing was done using the NextSeq500 Sequencer (Illumina, Inc., San Diego, CA, USA.) in combination with the NextSeq™ 500 High Output Kit (2 × 150 bp). Raw sequencing reads were converted to standard fastq format using bcl2fastq software 2.17.1.14 (Illumina, Inc.),

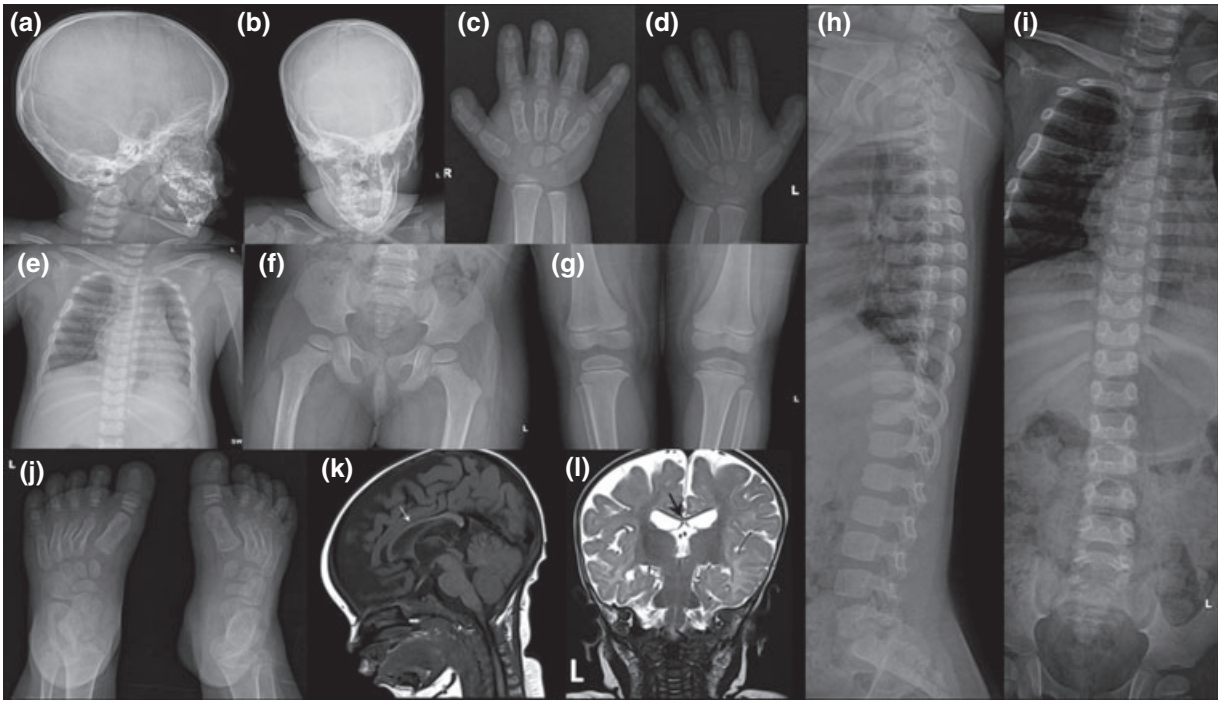

Fig. 2. Skeletal survey at age 3 years reveals an unremarkable skull (**a**, **b**), short and stubby metacarpals and phalanges, cone-shaped epiphysis of phalanges, hypoplastic distal phalanges and angel-shaped middle phalanges (**c**, **d**). Pelvis, hip joints, knee joints and lumbar vertebrae are unremarkable (**f–i**) and short metatarsals and phalanges in feet (j). Magnetic resonance imaging of the brain at 6 months of age shows hypoplastic corpus callosum (arrows; **k**, **l**).

and fed to an in-house developed pipeline for the analysis of whole-exome sequencing (WES) data, based on the 1000 Genomes Project (1000G) data analysis pipeline and GATK best practice recommendations, which includes widely used open source software projects. The short-reads are aligned to the GRCh37 (hg19) build of the human reference genome using bwa software with the mem algorithm. The alignments were converted to binary bam file format, sorted on the fly and de-duplicated. The primary alignment files for each sample are further refined and augmented by additional information following GATK best practices recommendations. Afterwards variant calling was performed on the secondary alignment files using three different variant callers (GATK HaplotypeCaller, freebayes and samtools). Variants were annotated using Annovar and in-house *ad hoc* bioinformatics tools. Alignments were visually verified with the Integrative Genomics Viewer v.2.3 and Alamut v.2.4.5 (Interactive Biosoftware, Rouen, France). Variant prioritization was performed without bias with a cascade of filtering steps. The pathogenic variant which was predicted as the causative variant was validated by Sanger sequencing in the proband and her parents (Further details of exome sequencing are provided in supporting information in Tables S2 and S3.).

Results and discussion

The phenotype of the present patient is consistent with a skeletal ciliopathy inheriting in an autosomal recessive manner and has significant overlap with cranioectodermal dysplasia type I (Sensenbrenner syndrome; MIM 218330), short rib polydactyly syndrome type 3 (MIM 613091) and asphyxiating thoracic dysplasia (MIM 263510) (5). Hence we expected a mutation in a gene encoding a protein in ciliary–centrosome complex. Chromosomal microarray revealed no copy number changes. A total of 16 regions of homozygosity representing 3.1% of the genome were observed to include IFT52 on chromosome 20 (Table S4). On WES of the trio, a homozygous nonsense pathogenic variant p.R142* (c.424C > T, NM_016004.3) was identified in the proband in exon 6 of *IFT52*. No other sequence variants of pathogenic significance were detected in any other gene known to be involved in the assembly and maintenance of cilia. This variant was not found in homozygous state in the 1000Genome project, the Exome Variant Server, the Exome Aggregation Consortium database, CentoMD and exome database of a local NGS service provider. This pathogenic variant is a nonsense mutation which introduces a premature stop codon resulting in the production of truncated protein which is very likely to undergo nonsense mediated mRNA decay. The parents are heterozygous carriers for this variant thus confirming the autosomal recessive mode of inheritance presumed by the pedigree analysis. *IFT52* encodes a 437 residue protein, IFT 52 homolog (Chlamydomonas) (GenBank ID: NM_016004.2).

IFT52 is a proline-rich protein and is also one of the components of the IFT-B core complex. The IFT-B complex consists of nine proteins in the core complex (IFT88, IFT81, IFT74, IFT70, IFT52, IFT46, IFT27,

IFT25 and IFT22) and five peripheral components (IFT172, IFT80, IFT57, IFT54 and IFT20). The core complex is further known to form a tetrameric sub complex (IFT88/70/52/46) and a pentameric subcomplex (IFT81/74/27/25/22). IFT52 is known to mediate the interactions of these two subcomplexes (6) and is evolutionarily conserved from unicellular algae to vertebrates, thus implying the importance of this protein in ciliogenesis (7). The orthologs of *IFT52* in lower organisms, such as Chlamydomonas (IFT52) (7), and OSM-6 in *Caenorhabditis elegans* (8) are well studied. IFT52 is located near the basal bodies of the cilia (9). It plays an important role in intraflagellar anterograde transport and is essential for flagellar assembly and stability (7). Defects in the IFT52 protein lead to disruption of the IFT-B complex, which in turn leads to the absence of ciliary/flagellar assembly. Mutated IFT52 protein in unicellular algae is known to produce bald cells (7). The IFT52 mutant mouse model exhibits tight mesencephalic flexure, neural tube defects, craniofacial development abnormalities, left-right and ventral midline defects and polydactyly depicting its role in perturbance of the normal embryological development including the function of cilia (10). The above mentioned data supports the hypothesis that our patient's phenotype could be caused by the truncating variant in IFT52. Additional functional studies or analysis of more patients with pathogenic variants are necessary to confirm that.

Supporting Information

Additional supporting information may be found in the online version of this article at the publisher's web-site.

Acknowledgements

We thank the family who cooperated with evaluation of the child and consented for participation in this study. The Department of Science and Technology, Government of India funded the project titled 'Application of autozygosity mapping and exome sequencing to identify genetic basis of disorders of skeletal development' (SB/SO/HS/005/2014).

References

1. Hildebrandt F, Benzing T, Katsanis N. Ciliopathies. N Engl J Med 2011: 364: 1533–1543.
2. Schmidts M. Clinical genetics and pathobiology of ciliary chondrodysplasias. J Pediatr Genet 2014: 3: 46–94.
3. Perrault I, Halbritter J, Porath JD et al. IFT81, encoding an IFT-B core protein, as a very rare cause of a ciliopathy phenotype. J Med Genet 2015: 52: 657–665.
4. Ziegler EE. 4.2 the CDC and euro growth charts. World Rev Nutr Diet 2015: 113: 295–307.
5. Bonafe L, Cormier-Daire V, Hall C et al. Nosology and classification of genetic skeletal disorders: 2015 revision. Am J Med Genet A 2015: 167: 2869–2892.
6. Taschner M, Kotsis F, Braeuer P et al. Crystal structures of IFT70/52 and IFT52/46 provide insight into intraflagellar transport B core complex assembly. J Cell Biol 2014: 207: 269–282.
7. Brazelton WJ, Amundsen CD, Silflow CD et al. The bld1 mutation identifies the Chlamydomonas osm-6 homolog as a gene required for flagellar assembly. Curr Biol 2001: 11: 1591–1594.
8. Collet J, Spike CA, Lundquist EA et al. Analysis of osm-6, a gene that affects sensory cilium structure and sensory neuron function in Caenorhabditis elegans. Genetics 1998: 148: 187–200.
9. Deane JA, Cole DG, Seeley ES et al. Localization of intraflagellar transport protein IFT52 identifies basal body transitional fibers as the docking site for IFT particles. Curr Biol 2001: 11: 1586–1590.
10. Liu A, Wang B, Niswander LA. Mouse intraflagellar transport proteins regulate both the activator and repressor functions of Gli transcription factors. Development (Cambridge, England) 2005: 132: 3103–3111.